Kinematics and Bifurcation of a Twofold-Symmetric Eight-bar Linkage

Z. Tang[1], D. Zlatanov[2] and J. Dai[1, 3]

[1]*Key Laboratory of Mechanism Theory and Equipment Design of Ministry of Education, Tianjin University, Tianjin 300072, China, e-mail: zhaotang@tju.edu.cn*
[2]*PMAR Robotics, University of Genoa, Genoa 16145, Italy, e-mail: zlatanov@dimec.unige.it*
[3]*Kings College London, University of London, London WC2R 2LS, UK, e-mail: jian.dai@kcl.ac.uk*

Abstract. The paper presents an eight-bar linkage derived from a rotatable kaleidocycle, a hinged ring of eight regular tetrahedra with revolute joint axes along common edges. A simplified derivation of the kinematics closure equation of the mechanism is proposed. The bifurcations of the two-dimensional configuration space of this two-degree-of-freedom linkage is analyzed by screw theory and the different modes of operation are described.

Key words: twofold-symmetric linkage, closure equation, bifurcation, singularity, kaleidocycle

1 Introduction

A kaleidocycle is a ring of an even number of tetrahedra hinged along common edges skew in every body [6, 9]. With eight or more tetrahedra, there is a continuous twisting inward-outward motion of the ring, displaying all the faces when the ring is viewed along its axis [4].

Kaleidocycles have been a known subject in recreational mathematics [2]. They are also of interest to mechanism theory [5, 8]. The equivalent linkage is a $2k$-bar hinged loop with skew revolute-joint axes in every link. For example, the kaleidocycle composed of six regular tetrahedra can be thought of as a realization of the threefold-symmetric Bricard linkage [1].

In this paper, we study a twofold-symmetric eight-bar linkage derived from the kaleidocycle consisting of eight regular tetrahedra. In Section 2, the closure equation of the eight-bar linkage is derived in a new and simplified way. The mobility and bifurcations [10] are analyzed in Section 3. The article concludes with Section 4.

2 Kinematics

The sketch of the Twofold-symmetric 8-bar linkage is shown in Fig. 1. It is composed of eight equal links connected with eight revolute joints. These joint axes are

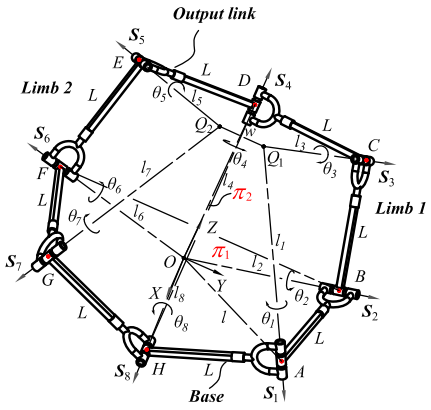

Fig. 1 Twofold-symmetric 8-bar linkage

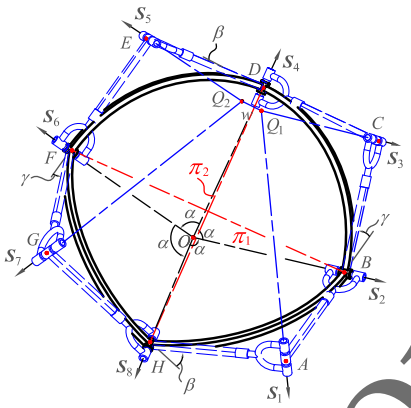

Fig. 2 Equivalent spherical four-bar linkage

denoted by $A, B, \ldots, H$ respectively. The axes of every two adjoining hinges are perpendicular, $A \perp B \perp C \perp \ldots \perp H \perp A$. When referring to a "link", e.g., AB, we will usually mean the common normal line or segment between two adjoining axes.

In the configuration in Fig. 1, the axes B, D, F, and H intersect at point O, while points Q_1 and Q_2 are the intersections of A, C and E, G, respectively.

The distance from O to link i is

$$l_{2i} = l_{2(i+1)} = L\tan\frac{\theta_{2i+1}}{2} \ (i = 1,2,3) \tag{1}$$

Thus,

$$l_2 = l_4 = l_6 = l_8 \ ; \ \theta_1 = \theta_3 = \theta_5 = \theta_7 \tag{2}$$

Suppose we now replace each link pair $HA-AB$, $BC-CD$, $DE-EF$, and $FG-GH$ by a single rigid body, HB, BD, DF and FH, respectively. (I.e., we fix the value of every second joint angle.) Then, the eight-bar can move as the spherical four-bar linkage shown in Fig. 2. As its four link lengths are identical, measured by the constant angle α, there are two perpendicular planes of symmetry $\pi_1(OBF)$ and $\pi_2(ODH)$. The points Q_1 and Q_2 are reflections in the plane π_2.

The joints values of the eight-bar in this spherical-four-bar mode can be given as

$$\begin{aligned} &\theta_1 = \theta_3 = \theta_5 = \theta_7 = \pi - \alpha \\ &\theta_2 = \theta_6 = \gamma \ ; \ \theta_4 = \theta_8 = \beta \end{aligned} \tag{3}$$

where β and γ are variable (and only one is independent).

For a general spherical four-bar linkage, it can be located on a spherical surface, as shown in Fig. 3, where these links are denoted by the arcs of AB, BC, CD and DA. Axes of their joints are OA, OB, OC and OD, and they intersect into the center O of the sphere. α_{ij} is the central angle of the arc link and ϕ_i is the angular displacement between two links.

The mathematical mapping between the parameters of geometric link and the angular displacements can be given as [7],

$$c_{12}(c_{34}c_{41} - c_4 s_{34} s_{41}) - s_{12}(c_1(c_4 c_{41} s_{34} + c_{34} s_{41}) - s_1 s_{34} s_4) - c_{23} = 0 \quad (4)$$

where
$s_{ij} = \sin\alpha_{ij},\ c_{ij} = \cos\alpha_{ij},\ s_i = \sin\phi_i,\ c_i = \cos\phi_i$

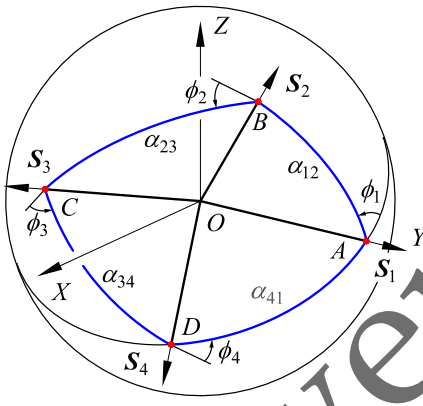

Fig. 3 Mode of spherical four-bar linkage

Because of symmetry, the geometric link parameters and the revolute joints variables of the spherical four-bar linkage in our case satisfy the following conditions:

$$\begin{aligned} \alpha_{41} = \alpha_{12} = \alpha_{23} = \alpha_{34} = \alpha \\ \phi_1 = \phi_3 = \beta\ ;\ \phi_2 = \phi_4 = \gamma \end{aligned} \quad (5)$$

Substituting Eq. (5) into Eq. (4), the closure equation of the 8-bar linkage can be written as

$$\sin^2\alpha(\sin\beta\sin\gamma - (\cos\beta + 1)(\cos\gamma + 1)\cos\alpha) = 0 \quad (6)$$

We now note that the initial configuration in Fig. 1 can be for a general value of α. For any given α and β, Eq. (6) determines the value of γ. (Equation (6) is symmetric in β and γ, so we can consider β to be the dependent variable.) We thus obtain a two-dimensional set of configurations, obtained from the initial one by varying α and β (or α and γ).

3 Mobility and Bifurcation

The distance between points Q_1 and Q_2 in Fig. 2 can be derived as

$$w = 2L\sin\frac{\beta}{2}(\cot\frac{\beta}{2} - \cot\frac{\gamma}{2}) \tag{7}$$

Let $w = 0$, i.e., Q_1 and Q_2 coincide and so the axes of A , C, E, and G intersect in one point. Then,

$$\beta = 0 \text{ or } \beta = \gamma \tag{8}$$

Substituting $\beta = \gamma$ into Eq. (6), the closure equation can be rewritten as

$$\sin^2\alpha(\sin^2\gamma - \cos\alpha(1+\cos\gamma)^2) = 0 \tag{9}$$

Therefore

$$\alpha = 0 \text{ or } \cos\alpha = \tan^2\frac{\gamma}{2} \tag{10}$$

When Q_1 and Q_2 coincide, the instantaneous mobility of the 8-bar linkage increases. Indeed, since each of the eight hinge axes passes through one of two points, the rank of the screw system spanned by all zero-pitch joint screws is at most five. Therefore the mobility of the loop is at least three, violating the conventional mobility formula for an 8-bar.

3.1 General configuration

We use a global reference frame $OXYZ$ (fixed in space but not in any of the rigid links) with the symmetry planes π_1 and π_2, chosen as OYZ and OXZ, respectively. In the figure, the OX and OY axes point down and to the right.

The screw coordinates of H and B, expressed in the global frame, are

$$\begin{aligned} \boldsymbol{S}_8 &= (m_1, 0, n_1, 0, 0, 0)^{\mathrm{T}} \\ \boldsymbol{S}_2 &= (0, m_2, n_2, 0, 0, 0)^{\mathrm{T}} \end{aligned} \tag{11}$$

We denote by $\boldsymbol{s}_i$ a unit vector directed as the axis of the i-joint screw $\boldsymbol{S}_i$. As adjoining axes are perpendicular, axis A is normal to axes B and H and so $\boldsymbol{s}_1 = \boldsymbol{s}_2 \times \boldsymbol{s}_8$. From (11), $\boldsymbol{s}_8 = [m_1, 0, n_1]^{\mathrm{T}}$ and $\boldsymbol{s}_2 = [0, m_2, n_2]^{\mathrm{T}}$. Hence,

$$\boldsymbol{S}_1 = (m_2 n_1, m_1 n_2, -m_1 m_2, -kp, kq, kr)^{\mathrm{T}} \tag{12}$$

where

$$p = m_1(m_2^2 + n_2^2 + n_1 n_2), \quad q = m_2(m_1^2 + n_1^2 + n_1 n_2), \quad r = m_1^2 n_2 - m_2^2 n_1$$

$$k = \frac{l}{\sqrt{m_1^2 + m_2^2 + (n_1 + n_2)^2}}$$

and l is the distance from O to axis A.

The coordinates of the eight joint screws can now be written as follows,

$$\mathbb{S}_{l1}\begin{cases}\boldsymbol{S}_1=(m_2n_1,\,m_1n_2,\,-m_1m_2,\,-kp,\,kq,\,kr)^{\mathrm{T}}\\ \boldsymbol{S}_2=(0,\,m_2,\,n_2,\,0,\,0,\,0)^{\mathrm{T}}\\ \boldsymbol{S}_3=(-m_2n_1,\,m_1n_2,\,-m_1m_2,\,-kp,\,-kq,\,-kr)^{\mathrm{T}}\\ \boldsymbol{S}_4=(-m_1,\,0,\,n_1,\,0,\,0,\,0)^{\mathrm{T}}\end{cases}$$
$$\mathbb{S}_{l2}\begin{cases}\boldsymbol{S}_5=(-m_2n_1,\,-m_1n_2,\,-m_1m_2,\,kp,\,-kq,\,kr)^{\mathrm{T}}\\ \boldsymbol{S}_6=(0,\,-m_2,\,n_2,\,0,\,0,\,0)^{\mathrm{T}}\\ \boldsymbol{S}_7=(m_2n_1,\,-m_1n_2,\,-m_1m_2,\,kp,\,kq,\,-kr)^{\mathrm{T}}\\ \boldsymbol{S}_8=(m_1,\,0,\,n_1,\,0,\,0,\,0)^{\mathrm{T}}\end{cases}\tag{13}$$

To analyze the mobility of the linkage we consider it as a parallel mechanism with two leg chains composed of joints, 1 to 4 and 5 to 8, respectively, and we follow the methodology described in [3]. The motion systems of this parallel mechanism are generated by the screws in (13), while the constraint systems are spanned by

$$\mathbb{S}^r_{l1}\begin{cases}\boldsymbol{S}^r_{11}=(0,\,-\dfrac{kr}{m_2n_1},\,\dfrac{kq}{m_2n_1},\,0,\,0,\,0)^{\mathrm{T}}\\ \boldsymbol{S}^r_{12}=(x,\,y,\,z,\,\dfrac{kl_2m_2n_1}{L},\,\dfrac{kl_2m_1n_2}{L},\,\dfrac{kl_2m_1m_2}{L})^{\mathrm{T}}\end{cases}$$
$$\mathbb{S}^r_{l2}\begin{cases}\boldsymbol{S}^r_{21}=(0,\,\dfrac{kr}{m_2n_1},\,\dfrac{kq}{m_2n_1},\,0,\,0,\,0)^{\mathrm{T}}\\ \boldsymbol{S}^r_{22}=(x,\,-y,\,z,\,-\dfrac{kl_2m_2n_1}{L},\,\dfrac{kl_2m_1n_2}{L},\,\dfrac{kl_2m_1m_2}{L})^{\mathrm{T}}\end{cases}\tag{14}$$

where

$$x=-\frac{km_1}{L},\quad y=-\frac{(k-l_2)m_2}{L},\quad z=\frac{k(n_1+n_2)-l_2n_2}{L},\quad l_2=\sqrt{l^2-L^2}$$

and L is the length of link AB.

This shows that $\dim(\mathbb{S}^r)=\mathrm{card}\,\langle\mathbb{S}^r\rangle=4$. So the mobility of the 8-bar linkage calculated from the mobility criterion in [3] is $m=8-6+4-4=2$.

3.2 Singular configurations

When the distance $|Q_1Q_2|$ equals to zero ($Q_1=Q_2$ as shown in Fig. 4), a spanning set of constraint screws of the 8-bar linkage can be derived as

$$\mathbb{S}^r_{l1} = \begin{cases} \boldsymbol{S}^r_{11} = (0,\, 0,\, \dfrac{kq}{m_2 n_1},\, 0,\, 0,\, 0)^{\mathrm{T}} \\ \boldsymbol{S}^r_{12} = (x,\, y,\, z,\, \dfrac{kl_2 m_2 n_1}{L},\, \dfrac{kl_2 m_1 n_2}{L},\, \dfrac{kl_2 m_1 m_2}{L})^{\mathrm{T}} \end{cases}$$
$$\mathbb{S}^r_{l2} = \begin{cases} \boldsymbol{S}^r_{21} = (0,\, 0,\, \dfrac{kq}{m_2 n_1},\, 0,\, 0,\, 0)^{\mathrm{T}} \\ \boldsymbol{S}^r_{22} = (x,\, -y,\, z,\, -\dfrac{kl_2 m_2 n_1}{L},\, \dfrac{kl_2 m_1 n_2}{L},\, \dfrac{kl_2 m_1 m_2}{L})^{\mathrm{T}} \end{cases} \tag{15}$$

Obviously, $\dim(\mathbb{S}^r) = 3$, $\mathrm{card}\,\langle \mathbb{S}^r \rangle = 4$. So in this configuration, the mobility of linkage, calculated as in [3], is $m = 8-6+4-3 = 3$.

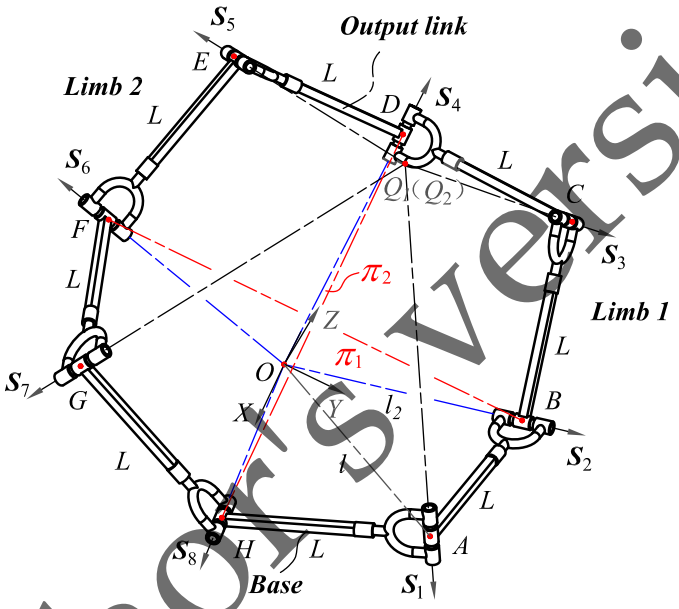

Fig. 4 8-bar linkage in a singular configuration

3.3 Discussion

Figure 5 illustrates the geometric nature of the bifurcation and the different modes of motion. There are two sheets (two-dimensional regions) of the configuration space where no links or joints coincide. In the first region, exemplified by Fig. 5(a), the axes of the revolute joints A, C, E and G intersect in one point. On the second sheet, Fig. 5(c), B, D, F and H are concurrent instead. On both sheets, the linkage has mobility two and two planes of symmetry. In the singular configuration, Fig. 5(b),

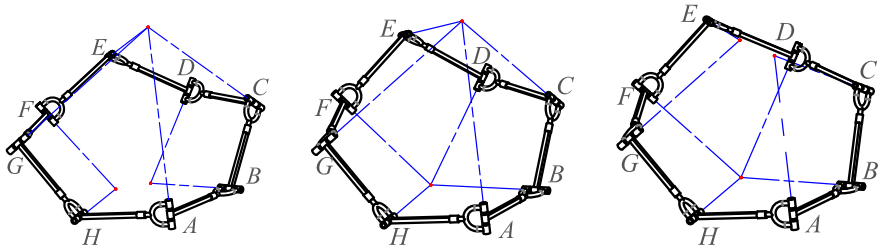

(a) Branch 1 (b) Singular configuration A (c) Branch 2

Fig. 5 Geometry of the bifurcation

the axes of two pairs of revolute joints intersect in one point simultaneously. The mobility of the 8-bar linkage changes to three with four symmetry planes.

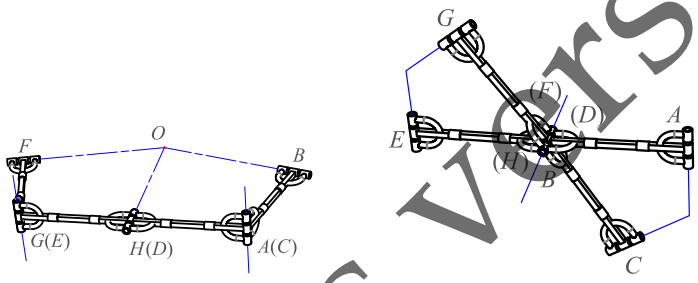

(a) Case 1: $\beta = 0$ (b) Case 2: $\alpha = 0$

Fig. 6 Two configurations with higher instantaneous mobility

From Eqs. (8) and (10), there are two other special cases: $\beta = 0$ and $\alpha = 0$. In the first, Fig. 6(a), the axes of revolute joints A, H and G are collinear with C, D and E, respectively, while B, D, F and H intersect in one point. In this configuration the mobility of the mechanism is four and the 8-bar linkage enters a 3-DOF region where it operates as a 3R serial chain. In the second case, Fig. 6(b), the axes B, D, F and H coincide. Also here the mechanism can now move as a 3R serial chain, but with coincident hinge axes.

In both cases, a general motion of the 3R serial chain reduces instantaneous mobility to three. While in some special cases, the mobility can stay the same if some condition is met. In Fig. 6(a), all the links should be coplanar and B, $D(H)$, F intersect in one point. In Fig. 6(b), there should be two perpendicular symmetric planes. In these cases, the mobility is always four and there exists a motion to come back to the non-overlapping configuration.

In both cases configurations with higher instantaneous mobility can be obtained when more axes become coincident. And these cases can be reproduced after any cyclic permutation of $A, B, \ldots, H$. These multiple regions have intersections in con-

figurations where even more revolute joints become coincident. The detailed analysis of the topology of the configuration space is rather complex and is omitted here due to lack of space. Moreover, in many of these cases the two-fold symmetry is not maintained. We should note, however, that although these configurations like the ones in Fig. 6 appear exotic, they constitute "most" of the points in the configuration space, as they form regions with dimensions higher than the "normal" 2-DOF operation modes.

4 Conclusions

This paper presents a two-fold symmetric 8-bar linkage evolved from a kaleidocycle with 8 equilateral tetrahedra. As there are four axes intersecting in one point at all time, the 8-bar linkage is treated as an equivalent spherical four-bar linkage. The closure equation is then obtained easily using methods of spherical four-bar analysis. Screw-system-based analysis identifies the singular configuration and reveals the bifurcation process. As the 8-bar linkage moves from one region of the configuration space to another, the four intersecting axes of revolute joints will switch.

Acknowledgements The authors wish to acknowledge the financial support received from the Natural Science Foundation of China No. 51535008 and International S&T Cooperation Program of China under No. 2014DFA70710.

References

1. Chen, Y., You, Z., Tarnai, T.: Threefold-symmetric Bricard linkages for deployable structures. International journal of solids and structures, 42(8), 2287-2301 (2005)
2. Cundy, H.M., Rollett, A.P.: Mathematical models. Tarquin (1981)
3. Dai, J.S., Huang, Z., Lipkin, H.: Mobility of overconstrained parallel mechanisms. Journal of Mechanical Design, 128(1): 220-229 (2006)
4. Fowler, P.W., Guest, S.D.: A symmetry analysis of mechanisms in rotating rings of tetrahedral. In: Proceedings of the Royal Society of London A: Mathematical, Physical and Engineering Sciences. The Royal Society, 461(2058), 829-1846 (2005)
5. Gan, W., Pellegrino, S.: Closed-loop deployable structures. In: Proceeding of the 44th AIAA/ASME/ASCE/AHS/ASC Structures, Structural Dynamics, and Materials Conference, Norfork, VA (2003)
6. Glassner, A.: Net results [3D graphics]. IEEE Computer Graphics and Applications. 17(4), 85-89 (1997)
7. He, S.I., Wang, S.E.: Study on Input/Output Equation for Spherical 4R Mechanism. Sci-Tech Information Development & Economy, 2: 083 (2011)
8. Safsten, C., Fillmore, T., Logan, A., Halverson, D., Howell, L.: Analyzing the Stability Properties of Kaleidocycles. Journal of Applied Mechanics, 83(5), 051001 (2016)
9. Schattschneider, D., Escher, M.C., Walker, W.: MC Escher kaleidocycles. Ballantine Books (1977)
10. Zlatanov, D., Bonev, I.A., Gosselin, C.M.: Constraint singularities of parallel mechanisms. In : ICRA. pp. 496-502 (2002)